Combined Adaptive Meshing Technique and a Characteristic-based Finite Volume Element Method for Solving Convection-Diffusion-Reaction Equation

Theeraek P.

Department of Mechanical Engineering, Faculty of Engineering, Burapha University, Chonburi, Thailand
E-mail address: patchareet@buu.ac.th

Abstract

A finite volume element method is combined with an adaptive meshing technique to solve the two-dimensional unsteady convection-diffusion-reaction equation. The characteristic-based scheme is used to derive the governing equation and then the finite volume method is employed to discretize the characteristic equation. Concept of the weighted residual method in the finite element method is applied to evaluate the gradient quantity at the cell faces. Finally, an adaptive meshing technique is applied to further improve the solution accuracy, and to minimize the computational time and computer memory requirement. The efficiency of the combined method is evaluated by the examples of pure-convection, convection-diffusion, convection-diffusion, and diffusion-reaction problems.

Keywords*: Characteristic-based scheme, Finite volume element method, Adaptive meshing technique*

1 Introduction

Numerical simulation for predicting the transport phenomena governed by the unsteady convection-diffusion-reaction equation is difficult due to the convection term. The flow behaviours usually contain steep gradients that require special treatment of numerical schemes. Most of the classical schemes suffer from the spurious oscillations, otherwise yields excessive numerical dispersion [1,2]. During the past decade, several stabilizing schemes have been developed for solving such difficulty. These schemes include the upwind-based methods [3,4], The characteristic Galerkin method [5], the Galerkin projected residual method [6], and the Taylor-Galerkin algorithm [7]. For both finite volume method and finite element method, the upwind based schemes have been employed widely for analysing convective-dominated flow. The characteristics Galerkin method is an attractive one due to its simple implementation and can be written in a fully explicit form for obtaining solution. At present, development of new numerical schemes for accurate solution of the convection-diffusion-reaction is still needed.

Computational techniques for solving the hyperbolic equation are generally classified into explicit and implicit (or semi-implicit) methods. The explicit method is simple and requires less computational time and computer memory than the implicit method. The disadvantage of the explicit method is it's constrain by the CFL condition in order to stabilize the spatial error from growing without bound. On the other hand, the implicit method provides more stable solution but a large time step may not be used because the solution accuracy degrades with time. The inversion of the coefficient matrix is another disadvantage because it is a time consumable process. Furthermore, a large block of memory is required for the coefficient matrix formation.

In this paper, the characteristic-based scheme is used to derive the two-dimensional unsteady convection-diffusion-reaction equation along the characteristic path. The cell-centered finite volume method is further discretized the equation using triangular meshes. The concept of weighted residuals method and the midpoint quadrature rule are applied to the unknown quantity gradient at the cell faces. Finally, an adaptive meshing technique is implemented to further improve the solution accuracy by refining meshes in the region of high solution gradients. Coarse meshes are constructed in the other regions to reduce the computational time and computer memory. The presentation of this paper starts from the explanation of the theoretical formulation and the

corresponding characteristic-based scheme in section 2. The finite volume element method for the characteristic equation and implementation of the adaptive meshing technique are explained in section 3 and 4, respectively. Performance of the combined method is examined by using four examples. These examples are: (1) Smith and Hutton problem, (2) the boundary layer flow problem, (3) the oblique inflow problem, and (4) the corner layer problem.

2 Characteristic-Based Scheme

The concept of characteristic-based scheme have been developed and extensively applied with the finite element method [8,9]. In this section the idea of the characteristic is applied to the two-dimensional unsteady convection-diffusion-reaction equation. The governing equation is,

$$\frac{\partial \phi}{\partial t} + \nabla \cdot \left(\boldsymbol{v}\phi - \varepsilon \nabla \phi \right) + \kappa \phi = q \tag{1}$$

where ϕ is the unknown scalar quantity, $\boldsymbol{v} = \boldsymbol{v}(\boldsymbol{x})$ is the given velocity, $\varepsilon \geq 0$ is the diffusivity parameter, and $q = q(\boldsymbol{x}, t)$ is the prescribed source term. Equation (1) is defined for the spatial domain $\boldsymbol{x} \in R$ where $\Omega \subset R^2$ and the time interval of $t \in (0, T)$ with $T > 0$. The initial condition is given by,

$$\phi(\boldsymbol{x}, 0) = \phi_0(\boldsymbol{x}) \tag{2}$$

This governing equation is subjected to the boundary conditions

$$\phi = g_D \text{ on } \partial\Omega_D \tag{3a}$$

$$\varepsilon \frac{\partial \phi}{\partial \boldsymbol{n}} = g_N \text{ on } \partial\Omega_N \tag{3b}$$

with $\partial\Omega = \partial\Omega_D \cup \partial\Omega_N$ and $\partial\Omega_D \cap \partial\Omega_N \neq 0$.

By changing the independent variable, $\boldsymbol{x}$, on the reference coordinate system to the moving coordinate system along their characteristic directions, $\boldsymbol{x}'$, such that

$$d\boldsymbol{x}' = d\boldsymbol{x} - \boldsymbol{v}dt \tag{4}$$

where $\boldsymbol{v}$ is the velocity of the moving coordinate system, let $\phi = \phi(\boldsymbol{x}', t)$ then,

$$\left.\frac{\partial \phi}{\partial t}\right|_{\boldsymbol{x}=const.} = -\boldsymbol{v} \cdot \nabla \phi + \left.\frac{\partial \phi}{\partial t}\right|_{\boldsymbol{x}'=const.} \tag{5}$$

with $\nabla \phi = \nabla' \phi$ (6)

and $\nabla \cdot (\varepsilon \nabla \phi) = \nabla \cdot (\varepsilon \nabla' \phi)$ (7)

By substituting Eqs. (5)-(7) into Eq.(1) and applying the divergence free assumption, $(\nabla \cdot \boldsymbol{v} = 0)$, the unsteady convection-diffusion-reaction along the characteristic can be rewritten as,

$$\frac{\partial \phi}{\partial t} - \nabla \cdot (\varepsilon \nabla \phi) + \kappa \phi = q \tag{8}$$

The time discretization of the above equation in the explicit form is obtained as,

$$\frac{1}{\Delta t}\left(\phi^{n+1} - \phi^n \Big|_{(\mathrm{x}-\Delta \mathrm{x})} \right) \approx \left(\nabla \cdot (\varepsilon \nabla \phi) - \kappa \phi + q \right)_{(\mathrm{x}-\Delta \mathrm{x})} \tag{9}$$

where Δt is the increment time period from n to $n+1$, and $\Delta \boldsymbol{x} = \bar{\boldsymbol{v}} \Delta t$ is the distance travelled by the particle which $\bar{\boldsymbol{v}}$ is the average velocity along the characteristic, that is

$$\bar{\boldsymbol{v}} = \frac{\boldsymbol{v}^{n+1} + \boldsymbol{v}^n \Big|_{(\boldsymbol{x}-\Delta \boldsymbol{x})}}{2} \tag{10}$$

Applying the Taylor's series expansion in space to the second term of the left-hand side, to all the right-hand side terms of Eq.(9), to the second term of the right-hand side of Eq.(10), and further approximate half time step velocity, $\boldsymbol{v}^{n+1/2} = \frac{\boldsymbol{v}^{n+1} + \boldsymbol{v}^n}{2}$, as,

$$\boldsymbol{v}^{n+1/2} \approx \boldsymbol{v}^n + \mathrm{O}(\Delta t) \tag{11}$$

Finally, an explicit scheme can be rewritten as,

$$\begin{aligned} \phi^{n+1} - \phi^n = & -\Delta t \left(\nabla \cdot (\boldsymbol{v}\phi - \varepsilon \nabla \phi) + \kappa \phi - q \right) \\ & + \frac{\Delta t^2}{2} \nabla \cdot \left(\boldsymbol{v} (\boldsymbol{v} \cdot \nabla \phi) + \kappa \phi - q \right) \end{aligned} \tag{12}$$

3 Finite volume element formulation

The finite volume element technique, herein, is based on the discretization on the cell-centered method. The computational domain is discretized into the non-overlapping triangular control volumes, $\Omega_i \in \Omega$, $i = 1, 2, \ldots, N$, such that $\Omega = \bigcup_{i=1}^{N} \Omega_i, \Omega_i \neq 0$, and $\Omega_i \cap \Omega_j = 0$ if $i \neq j$. Equation (12) is integrated over the control volume Ω_i as,

$$\int_{\Omega_i}\phi^{n+1}d\boldsymbol{x}=\int_{\Omega_i}\phi^{n}d\boldsymbol{x} -\Delta t\int_{\Omega_i}\left(\nabla\cdot\left(\boldsymbol{v}\phi-\varepsilon\nabla\phi\right)+\kappa\phi-q\right)d\boldsymbol{x} +\frac{(\Delta t)^2}{2}\int_{\Omega_i}\left(\nabla\cdot\left(\boldsymbol{v}\left(\boldsymbol{v}\cdot\nabla\phi\right)+\kappa\phi-q\right)\right)d\boldsymbol{x} \tag{13}$$

The approximations to the cell average of ϕ over control volume Ω_i at time t^n and t^{n+1} are represented by,

$$\phi_i^{n+1}=\frac{1}{|\Omega_i|}\int_{\Omega_i}\phi\left(\boldsymbol{x},t^{n+1}\right)d\boldsymbol{x} \tag{14a}$$

$$\phi_i^{n}=\frac{1}{|\Omega_i|}\int_{\Omega_i}\phi\left(\boldsymbol{x},t^{n}\right)d\boldsymbol{x} \tag{14b}$$

where $|\Omega_i|$ is the measure of cell i. Applying the divergence theorem to the convection-diffusion term yield,

$$\phi_i^{n+1}=\phi_i^{n} -\frac{\Delta t}{|\Omega_i|}\left[\int_{\partial\Omega_i}\boldsymbol{n}_i(\upsilon)\cdot\left(\boldsymbol{v}(\upsilon)\phi(\upsilon,t)-\varepsilon\nabla\phi(\upsilon,t)\right)d\upsilon\right] -\frac{\Delta t}{|\Omega_i|}\left[\int_{\Omega_i}\kappa\phi(\boldsymbol{x},t)-q(\boldsymbol{x},t)d\boldsymbol{x}\right] +\frac{(\Delta t)^2}{2|\Omega_i|}\left[\int_{\partial\Omega_i}\left(\boldsymbol{n}_i(\upsilon)\cdot\boldsymbol{v}(\upsilon)\right)\left(\boldsymbol{v}(\boldsymbol{x})\cdot\nabla\phi(\boldsymbol{x},t)\right)d\upsilon\right] +\frac{(\Delta t)^2}{2|\Omega_i|}\left[\int_{\partial\Omega_i}\left(\boldsymbol{n}_i(\upsilon)\cdot\boldsymbol{v}(\upsilon)\right)\left(\kappa\phi(\boldsymbol{x},t)-q(\boldsymbol{x},t)\right)d\upsilon\right] \tag{15}$$

For an arbitrary triangular control volume, the flux integral over $\partial\Omega_i$ appearing on the right-hand side of Eq.(15) could be approximated by summation of the fluxes passing through the three adjacent cell faces. By applying the quadrature integration formula, the flux integral over $\partial\Omega_i$ in the above equation can be approximated by,

$$\int_{\partial\Omega_i}\boldsymbol{n}_i(\upsilon)\cdot\left(\boldsymbol{v}(\upsilon)\phi(\upsilon,t)-\varepsilon\nabla\phi(\upsilon,t)\right)d\upsilon =\sum_{j=1}^{3}|\Gamma_{ij}|\boldsymbol{n}_{ij}\cdot\left(\boldsymbol{v}_{ij}\phi_{ij}\left(t^n\right)-\varepsilon\nabla\phi_{ij}\left(t^n\right)\right) \tag{16}$$

and

$$\int_{\partial\Omega_i}\left(\boldsymbol{n}_i(\upsilon)\cdot\boldsymbol{v}(\upsilon)\right)\left(\boldsymbol{v}(\boldsymbol{x})\cdot\nabla\phi(\boldsymbol{x},t)+\kappa\phi(\boldsymbol{x},t)-q(\boldsymbol{x},t)\right)d\upsilon =\sum_{j=1}^{3}|\Gamma_{ij}|\left(\boldsymbol{n}_{ij}\cdot\boldsymbol{v}_{ij}\right)\left(\boldsymbol{v}_i\cdot\nabla\phi_i\left(t^n\right)+\kappa\phi_i\left(t^n\right)-q_i\left(t^n\right)\right) \tag{17}$$

where subscript ij indicate the quantity evaluated at midpoint of the cell face between the two adjacent, Ω_i and Ω_j. The segment of the boundary $\partial\Omega_i$, Γ_{ij}, is defined by $\partial\Omega_i=\bigcup_{j=1}^{3}\Gamma_{ij}$ and $\Gamma_{ij}=\partial\Omega_i\cap\partial\Omega_j$. The velocity vector, $\boldsymbol{v}_{ij}$, and the unknown quantity, $\phi_{ij}\left(t^n\right)$, are also evaluated at midpoint of the cell face.

Integration of the reaction and source terms could be approximated by the cell average over the control volume, then

$$\int_{\Omega_i}\kappa\phi(\boldsymbol{x},t)d\boldsymbol{x}=|\Omega_i|\kappa\phi_i\left(t^n\right) \tag{18}$$

$$\int_{\Omega_i}q(\boldsymbol{x},t)d\boldsymbol{x}=|\Omega_i|q_i\left(t^n\right) \tag{19}$$

By substituting Eqs.(16)-(19) into Eq.(15), an explicit finite volume scheme for solving Eq.(1) is obtained as,

$$\phi_i^{n+1}=\phi_i^{n}-\frac{\Delta t}{|\Omega_i|}\sum_{j=1}^{3}|\Gamma_{ij}|\boldsymbol{n}_{ij}\cdot\left[\left(\boldsymbol{v}_{ij}\phi_{ij}^{n}-\varepsilon\nabla\phi_{ij}^{n}\right) -\frac{\Delta t}{2}\boldsymbol{v}_{ij}\left(\boldsymbol{v}_i\cdot\nabla\phi_i^{n}+\kappa\phi_i^{n}-q_i^{n}\right)\right] -\Delta t\left(\kappa\phi_i^{n}-q_i^{n}\right) \tag{20}$$

where the quantities at time t^n are defined by $\phi_{ij}^{n}=\phi_{ij}\left(t^n\right)$, $\phi_i^{n}=\phi_i\left(t^n\right)$, and $q_i^{n}=q_i\left(t^n\right)$.

The unknown quantity at the cell face, ϕ_{ij}^n , can be approximated by applying Taylor's series expansion according to the upwind direction as,

$$\phi_{ij}^n = \begin{cases} \phi_i^n + \left(\boldsymbol{x}_{ij} - \boldsymbol{x}_i\right)\cdot\nabla\phi_i^n & ,\boldsymbol{v}_{ij}\cdot\boldsymbol{n}_{ij} \geq 0 \\ \phi_j^n + \left(\boldsymbol{x}_{ij} - \boldsymbol{x}_j\right)\cdot\nabla\phi_j^n & ,\boldsymbol{v}_{ij}\cdot\boldsymbol{n}_{ij} < 0 \end{cases} \tag{21}$$

In this paper, the concept of finite element method is applied to determine the gradient quantities. The gradient at the centre of control volume, $\nabla\phi_i^n$, is determined by the weighted residuals method and is assumed to be linearly distributed over cell Ω_i,

$$\nabla\phi_i^n = \sum_{k=1}^{3} N_k(\boldsymbol{x})\nabla\phi_k^n \tag{22}$$

where $N_k(\boldsymbol{x})$ denotes the linear interpolation functions for the triangular cell and $k = 1,2,3$ represent the control volume vertices. By applying the standard Galerkin method and the Gauss's theorem to Eq.(22), the gradient quantities at a grid point are obtained as,

$$\nabla\phi_{J,i}^n = \boldsymbol{M}^{-1}\left[\int_{\partial\Omega_i} n_i(\upsilon)N_J(\upsilon)\phi_i^n d\upsilon - \int_{\Omega_i}\frac{\partial N_J(\boldsymbol{x})}{\partial\boldsymbol{x}}\phi_i^n d\boldsymbol{x}\right] \tag{23}$$

where $\boldsymbol{M}$ is the lumped mass matrix and $\nabla\phi_{J,i}^n$ are the contributions of the gradient quantities in the control volume Ω_i to the gradient quantities at the grid point J. In order to determine the total gradient quantities at the grid point J, Eq.(23) is applied to all the volumes surrounding it such that,

$$\nabla\phi_J^n = \sum_{i=1}^{NV}\nabla\phi_{J,i}^n \tag{24}$$

where NV is the number of the surrounding triangular cells. The gradient quantities at the cell face, $\nabla\phi_{ij}^n$, is then determined by applying the midpoint quadrature integration rule along the edge that connects grid point I and J.

To ensure the stability of an explicit scheme on a triangular mesh, the CFL-like stability criterion must be fulfilled. In this paper, the permissible time step within each cell is determined from

$$\Delta t = C\min_i\left[\frac{|\Omega_i|}{\max_{j=1,2,3}|\boldsymbol{v}_{n,ij}|}, \frac{|\Gamma_i^c|^2}{2\varepsilon}\right] \tag{25}$$

where $\boldsymbol{v}_{n,ij}$ is the normal velocity at Γ_{ij}, Γ_i^c, is the characteristic length of cell i, and $0 < C \leq 1$.

4 Adaptive meshing technique

The concept of the adaptive meshing technique is to generate an entirely new mesh based on the solution obtained from an earlier mesh [10,11]. The new mesh consists of small cells in the regions with large change in solution gradients and larger cells in the other regions where the change in solution gradients are small. The adaptive meshing procedure employed in this paper is based on the advancing front technique for which the grid points are firstly generated along the outer domain boundary. Triangular elements are then constructed from these grid points and gradually propagate into the domain interior. The mesh construction is complete when the domain interior is fulfilled with all triangular cells. To determine proper element sizes at different locations in the flow field, the solid-mechanics concept for finding the principal stresses from a given state of stresses at appoint is employed. The second derivatives of the unknown quantity ϕ with respect to global coordinates $\boldsymbol{x}$ can be computed in the principal directions $\boldsymbol{X}$ as,

$$\begin{bmatrix} \frac{\partial^2\phi}{\partial x^2} & \frac{\partial^2\phi}{\partial x\partial y} \\ \frac{\partial^2\phi}{\partial x\partial y} & \frac{\partial^2\phi}{\partial y^2} \end{bmatrix} \Rightarrow \begin{bmatrix} \frac{\partial^2\phi}{\partial X^2} & 0 \\ 0 & \frac{\partial^2\phi}{\partial Y^2} \end{bmatrix} \tag{26}$$

The second derivatives of the unknown quantity ϕ with respect to coordinates $\boldsymbol{x}$ are determined by using the concept of weighted residuals method. For example, to determine $\frac{\partial^2\phi}{\partial x^2}$, the computed solution ϕ_i, is assumed to be linearly over cell Ω_i as

$$\phi_i = \sum_{k=1}^{3} N_k(\boldsymbol{x})\phi_k \tag{27}$$

where $N_k(\boldsymbol{x})$ denotes the linear interpolation functions for the triangular cell and $k = 1,2,3$ are the control volume vertices. By applying the standard

Galerkin method, the first derivative can be derived and determined from

$$\left.\frac{\partial \phi}{\partial x}\right|_{J,i} = \boldsymbol{M}^{-1} \int_{\Omega_i} N_J d\boldsymbol{x} \left.\frac{\partial \phi}{\partial x}\right|_i \tag{28}$$

where $\boldsymbol{M}$ is the lumped mass matrix and $\left.\frac{\partial \phi}{\partial x}\right|_{J,i}$ is the contribution of the first derivative quantity at the grid point J. By applying the same procedure, the second derivative is,

$$\left.\frac{\partial^2 \phi}{\partial x^2}\right|_{J,i} = \boldsymbol{M}^{-1} \int_{\Omega_i} N_J d\boldsymbol{x} \left.\frac{\partial^2 \phi}{\partial x^2}\right|_i \tag{29}$$

Then, the second derivative at the grid point J is determined from,

$$\left.\frac{\partial^2 \phi}{\partial x^2}\right|_{J} = \sum_{i=1}^{NV} \left.\frac{\partial^2 \phi}{\partial x^2}\right|_{J,i} \tag{30}$$

where NV is the number of the surrounding triangular cells.

The second derivatives are used to determine the proper mesh sizes, $h_i, i = 1,2$ in the two principal directions using condition,

$$h_i{}^2 \lambda_i = h_{\min}{}^2 \lambda_{\max} = \text{constant} \tag{31}$$

where $\lambda_i, i = 1,2$ are the second derivatives of the unknown quantity in the two principal directions of the cell considered. $h_{\min}$ is the minimum characteristic length and $\lambda_{\max}$ is the maximum principal quantity for the entire model.

Base on the above condition, the cell sizes are generated according to the given minimum cell size, $h_{\min}$. Specifying too small $h_{\min}$ may result in a model with an excessive number of cells. On the other hand, specifying too large $h_{\min}$ may result inadequate solution accuracy. These factors must be considered prior to generating a new mesh.

5 Numerical Examples

To evaluate the performance of the finite volume element method and to demonstrate the solution improvement after combining it with the adaptive meshing technique, four examples of pure convection, convection-diffusion, convection-reaction, and diffusion-reaction problems are performed. These examples are: (1) Smith and Hutton problem, (2) The boundary layer problem, (3) The oblique inflow problem, (4) The corner layer problem

5.1 *Smith and Hutton problem*

The first example is a pure convection problem in a rectangular domain $\Omega = (-1,0)\times(1,1)$ [12]. The velocity field is given by $\boldsymbol{v} = \left(2y\left(1-x^2\right), -2x\left(1-y^2\right)\right)$ and the initial condition $\phi_0(\boldsymbol{x})$ is set to be zero. The boundary condition is prescribed in a step function as shown in Figure 1.

The computation starts from using an unstructured mesh with 1886 uniform triangular cells. Figure 2(a)-(b) shows the initial and the third adaptive meshes with their computed solutions. The comparison of the exact and the computed solutions at the outflow boundary are shown in Figure 3. The comparison shows the computed solutions from the third adapted mesh are consistent with the exact solutions.

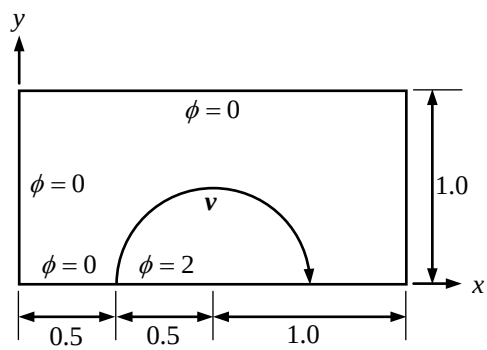

Figure 1: Physical domain of Smith and Hutton Problem.

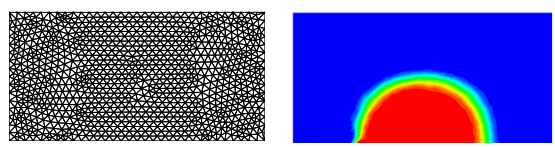

(a) Initial mesh and solution

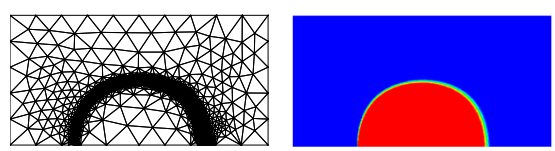

(b) Third adaptive mesh and solution

Figure 2: Adaptive meshes and computed solutions of Smith and Hutton problem.

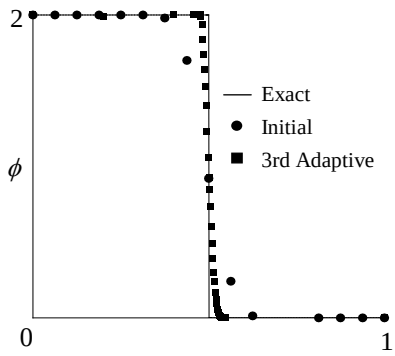

Figure 3: Comparisons of the exact and computed solutions of Smith and Hutton problem.

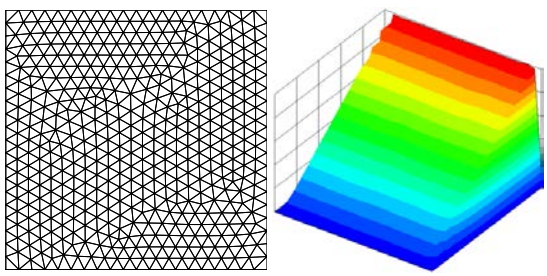

(a) Initial mesh and solution

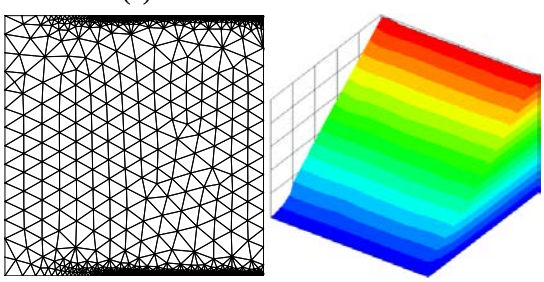

(b) Third adaptive mesh and solution

Figure 4: Adaptive meshes and computed solutions of the boundary layer problem.

5.2 *The boundary layer problem*

The second example is a convection-diffusion problem for determining the behaviour of the boundary layer flow in a square domain $\Omega = (0,1)\times(0,1)$ [13]. The initial condition, $\phi_0(\boldsymbol{x})$, is set to be zero and the velocity field is given by $\boldsymbol{v} = (1,0)$. The small diffusion coefficient is specified as $\varepsilon = 10^{-4}$ with the source term of $q = 1$. The boundary condition is set to be zero along the upper, lower, and the left-hand side of the computational domain.

The test case is performed until the final time step is equal to 2. The computation starts from using an unstructured mesh with 884 uniform triangular cells (20 cells along each boundary). Figure 4(a)-(b) shows the initial and the third adaptive meshes with their computed solutions at the final time by using the three-dimensional contour plots. The maximum and minimum cell sizes of the third adaptive mesh are 0.1 and 0.002, respectively. Oscillation of the solution obtained from the coarse initial mesh occurs along the edge of the profile. This oscillation disappears after the second mesh adaptation.

5.3 *The oblique inflow problem*

The third example is an oblique inflow convection-reaction problem [9]. The computational is a unit square of $\Omega = (0,1)\times(0,1)$, and the initial condition, $\phi_0(\boldsymbol{x})$, is set to be zero. The source term, q, is given as a constant of 1. The steady velocity field is given by $\boldsymbol{v} = (v\cos(\pi/3), v\sin(\pi/3))$. Two different cases have been considered corresponding to dominant convection and reaction, respectively. These cases are:

1. $v = 1, \kappa = 10^{-4}$ for convection-dominated problem,

2. $v = 10^{-4}, \kappa = 1$ for reaction-dominated problem

The computation starts from using the same initial unstructured mesh as shown in the previous example. The initial and adaptive meshes with their corresponding steady-state solutions for case 1 are shown in Figures 5(a)-(b), respectively. The analysis is performed until the final time step is equal to 2. With such a small reaction effect, the solution profile flows across the domain with an increasing amount of its height until it approaches the outflow boundaries. The oscillation occurs along the fronts of the profile from using of the coarse initial mesh and diminishes after the second mesh adaptation. For case 2 where the reaction is dominated, the solution profile also flows across the domain with an increasing amount of its uniform height throughout the domain. This latter case is performed until the final time step is equal to 1. Figure 6(a)-(b) shows the initial and the third adaptive meshes with their corresponding solutions at the final time by using the three-dimensional contour plots. Spurious oscillations occur along the profile fronts because of the coarse mesh. Such oscillations disappear after the meshes are adapted with small cells along the fronts of the profiles.

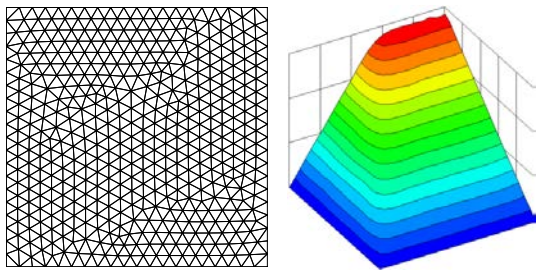

(a) Initial mesh and solution

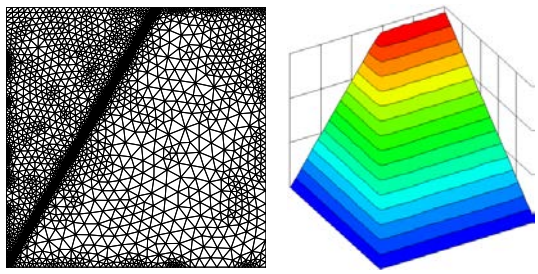

(b) Third adaptive mesh and solution

Figure 5: Adaptive meshes and computed solutions of the oblique inflow (convection dominated) problem.

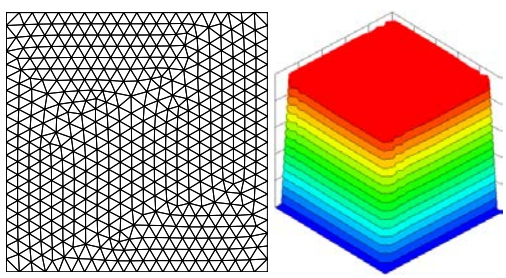

(a) Initial mesh and solution

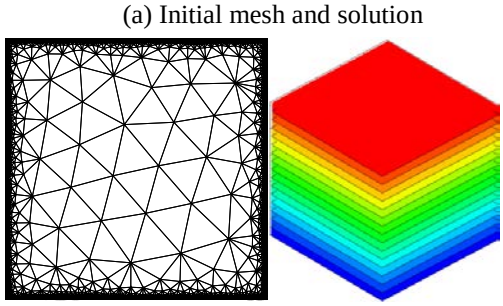

(b) Third adaptive mesh and solution

Figure 6: Adaptive meshes and computed solutions of the oblique inflow (reaction dominated) problem.

5.4 *The corner layer problem*

The last example is singularly perturbed diffusion-reaction problem [14]. The computational domain is a unit square of $\Omega = (0,1)\times(0,1)$. The initial condition, $\phi_0(\boldsymbol{x})$, and the Dirichet boundary condition, $\phi(\boldsymbol{x})$, are prescribed as zero. The source term is given by

$$q = 20\left(x^2 + y^2\right) + 4 \tag{32}$$

The diffusion coefficient is specified as $\varepsilon = 10^{-3}$, and the reaction coefficient, κ,is set to be 2. This example is performed until the final time step is equal to 5. The solution profile exhibits very sharp boundary layer along the upper sides and the right-hand side. If the meshes in these regions are not fine enough, oscillated solution may occur along these boundaries, especially at the corner point (1,1). In order to suppressing such oscillation, the Barth and Jespersen limiter function [15] is imposed as follows:

$$\alpha_{\Omega_i}^{BJ} = \min_{\forall \Gamma_{ij} \in \partial\Omega_i} \begin{cases} \dfrac{\phi_i^{\max} - \phi_i^n}{\bar{\phi}_{ij}^n - \phi_i^n}, & \bar{\phi}_{ij}^n > \phi_i^{\max} \\ \dfrac{\phi_i^{\min} - \phi_i^n}{\bar{\phi}_{ij}^n - \phi_i^n}, & \bar{\phi}_{ij}^n < \phi_i^{\min} \\ 1, & \text{otherwise} \end{cases} \tag{33}$$

where $\phi_i^{\max} \equiv \max_{\forall \Gamma_{ij} \in \partial\Omega_i} \left(\phi_i, \phi_j\right)$, $\phi_i^{\min} \equiv \min_{\forall \Gamma_{ij} \in \partial\Omega_i} \left(\phi_i, \phi_j\right)$, and $\bar{\phi}_{ij}^n = \phi_{ij}^n - \dfrac{\Delta t}{2}\left(\boldsymbol{v}_i \cdot \nabla \phi_i^n\right)$.

The computational domain is initially performed by using an unstructured mesh with 884 uniform triangular cells (20 cells along each boundary). As the meshes are adapted corresponding to the computed solutions, small cell sizes are generated in the region of high solution gradients along the upper sides and the right-hand side. Figure 7(a)-(b) shows the initial and the third adaptive meshes with their corresponding solutions at the final time. The computed solution obtained from the initial mesh shows some oscillations without overshooting along the boundary. Oscillations decrease as the meshes are adapted with the solutions.

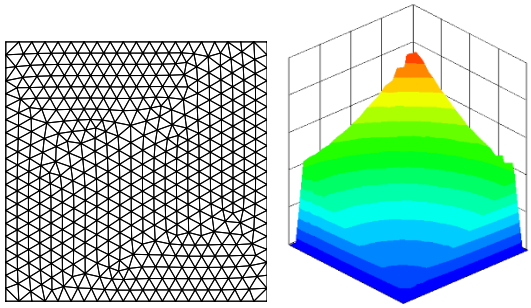

(a) Initial mesh and solution

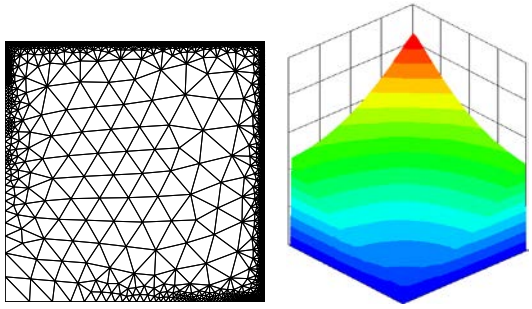

(b) Third adaptive mesh and solution

Figure 7: Adaptive meshes and computed solutions of the corner layer problem.

6 Conclusions

This paper presents a combination of an adaptive meshing technique and a characteristic-based finite volume element method for solving the two-dimensional unsteady convection-diffusion-reaction equation. The computations are performed on unstructured triangular meshes based on cell-centered method. The theoretical formulation of the proposed method and the concept of adaptive meshing technique were explained in details. The governing equation was derived by the characteristic-based scheme and discretized by the finite volume method. The weighted residuals concept of the finite element method was implemented to estimate the gradient quantities at cell faces. The adaptive meshing technique generates small clustered cells in the regions of high solution gradients to increase the solution accuracy. Larger cell sizes are generated in the other regions to reduce the computational time and computer memory. Four examples were used to evaluate performance of the proposed method. Results show that the combined method provides improved accuracy and decrease oscillated solution with the adaptive meshes.

References

[1] Kruganov A. and Tadmor E., 2000. New High-Resolution Central Schemes for Nonlinear Conservation Laws and Convection-Diffusion Equations, *Journal of Computational Physics*, 160: 241-282.

[2] Wang H. and Liu J., 2001. Development of CFL-free Explicit Schemes for Multidimensional Advection-Reaction Equations, *SIAM Journal of scientific computing*, 23: 1418-1438.

[3] Leveque R. J., 2005. *Finite Volume Methods for Hyperbolic Problems*, 3rd Edition, Cambridge University Press.

[4] Malatip A., Wansophark N. and Dechaumphai P., 2009. Combined Streamline Upwind Petrov Galerkin Method and Segregated Finite Element Algorithm for Conjugated Heat Transfer Problems, *Journal of Mechanical Science and Technology*, 20: 1741-1752.

[5] Zienkiewicz O. C. and Taylor R. L., 2000. *The Finite Element Method Volume 3: Fluid Dynamics*, 5th Edition, Butterworth-Hienemann, Burlington, MA.

[6] Carmo E. G. D., Alvarez G. B., Rochinha F. A. and Loula A. F. D., 2008. Galerkin Projected Residual Method Applied to Diffusion-Reaction Problems: The Streamline and Approximate Upwind/Petrov-Galerkin Method, *Computer Methods in Applied Mechanics and Engineering*, 197: 4559-4570.

[7] Peraire J., Peiro J., Formaggia K., Morgan K. and Zienkiewicz O. C., 1995. Finite Element Euler Computations in Three Dimensions, *International Journal for Numerical Methods in Fluids*, 26: 2135-2159.

[8] Zienkiewicz O. C. and Codina R., 1995. A General Algorithm for Compressible and Incompressible Flow-Part I. The Split, Characteristic-based Scheme, *International Journal for Numerical Methods in Fluids*, 20: 869-885.

[9] Phongthanapanich S. and Dechaumphai P., 2008. A Characteristic-based Finite Volume Element Method for Convection-Diffusion-Reaction Equation, *Transactions of the CSME*, 32: 549-560.

[10] Dechaumphai P., 1995. Adaptive Finite Element Technique for Heat Transfer Problems, *Journal of Energy Heat and Mass Transfer*, 17: 87-94.

[11] Peraire J., Vahjdati M., Morgan K. and Zienkiewicz O. C., 1987. Adaptive Remeshing

for Compressible Flow Computation, *Journal of Computational Physics*, 72: 449-466.

[12] Darwish M. S. and Moukalled F., 2003. TVD Schemes for Unstructured Grids, *International Journal of Heat and Mass Transfer*, 46: 599-611.

[13] Carmo E. G. D. and Alvarez G. B., 2003. A New Stabilized Finite Element Formulation for Scalar Convection-Diffusion Problems: The Streamline and Approximate Upwind/Petrov-Galerkin Method, *Computer Methods in Applied Mechanics and Engineering*, 192: 3379-3396.

[14] Phongthanapanich S. and Dechaumphai P., 2009. Combined Finite Volume Element Method for Singularly Perturbed Reaction-Diffusion Problems, *Applied Mathematics and Computation*, 209: 177-185.

[15] Barth T. and Ohlberger M., 2004. *Encyclopedia of Computational Mechanics Volume 1: Fundamentals*, John Wiley and Sons.